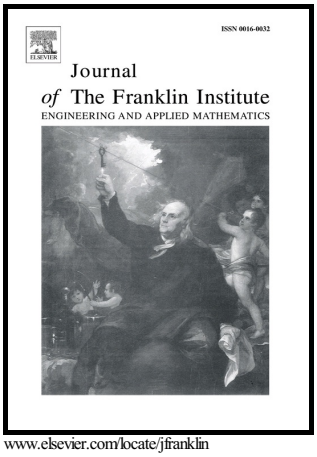

www.elsevier.com/locate/jfranklin

Stability of Markov jump systems with quadratic terms and its application to RLC circuits

Alessandro N. Vargas, Gisela Pujol, Leonardo Acho

PII: S0016-0032(15)30180-0
DOI: http://dx.doi.org/10.1016/j.jfranklin.2016.08.031
Reference: FI2739

To appear in: *Journal of the Franklin Institute*

Received date: 27 July 2015
Revised date: 25 July 2016
Accepted date: 26 August 2016

Cite this article as: Alessandro N. Vargas, Gisela Pujol and Leonardo Acho, Stability of Markov jump systems with quadratic terms and its application t RLC circuits, *Journal of the Franklin Institute* http://dx.doi.org/10.1016/j.jfranklin.2016.08.031

Stability of Markov jump systems with quadratic terms and its application to RLC circuits☆

Alessandro N. Vargas[a,1,*], Gisela Pujol[b], Leonardo Acho[b]

[a] *Universidade Tecnológica Federal do Paraná, UTFPR, Av. Alberto Carazzai 1640, 86300-000 Cornelio Procópio-PR, Brazil.*
[b] *CoDAlab (Control, Dynamics and Applications), Departament de Matemàtica Aplicada III, Universitat Politècnica de Catalunya, Comte d'Urgell, 187, 08036 Barcelona, Spain.*

Abstract

The paper presents results for the second moment stability of continuous-time Markov jump systems with quadratic terms, aiming for engineering applications. Quadratic terms stem from physical constraints in applications, as in electronic circuits based on resistor (R), inductor (L), and capacitor (C). In the paper, an RLC circuit supplied a load driven by jumps produced by a Markov chain—the RLC circuit used sensors that measured the quadratic of electrical currents and voltages. Our result was then used to design a stabilizing controller for the RLC circuit with measurements based on that quadratic terms. The experimental data confirm the usefulness of our approach.

Keywords: Stochastic systems; Quadratic systems; Markov jump systems; Stability; Electronic circuits.

1. Introduction

Systems subject to Markovian jumps have received attention in recent years because of their potential for representing processes subject to abrupt variations—see, for instance, some recent applications in economics [6], [16], robotics [21], and direct current (DC) motors [17, 19, 20, 25]. In the linear context, recent contributions for Markov jump systems can be found in the monographs [3, 7] and in the papers [5, 9, 18, 22, 26, 27, 28, 29]; for the nonlinear counterpart, contributions can be found in [14, 23, 24, 32], just to cite a few.

Although characterizing the stability of nonlinear Markov jump systems has been a topic of intensive research [14, 23, 24, 31], little attention has been paid to the stability of quadratic Markov jump systems. In reality, to the best of the authors' knowledge,

☆Research supported in part by the Spanish Ministry of Economy and Competitiveness through the research projects DPI2015-64170-R/MINECO/FEDER, DPI2011-25822,DPI2015-64170-R/MINECO/FEDER; by the Government of Catalonia (Spain) through 2014SGR859; and by the Brazilian agencies FAPESP Grants 03/06736-7; CNPq Grant 304856/2007-0; and CAPES Grant Programa PVE 88881.030423/2013-01.

*Corresponding author
Email address: avargas@utfpr.edu.br (Alessandro N. Vargas)

this paper is the first to consider quadratic terms for Markov jump systems. Presenting easy-to-check conditions to guarantee the stability of such systems represents the main contribution of this paper.

To clarify our findings, we now formalize the quadratic Markov jump system under study. Let $(\Omega, \mathcal{F}, \{\mathcal{F}_t\}, P)$ be a fixed, filtered probability space governing the following Itô stochastic differential equation with Markov jumps:

$$\mathrm{d}x(t) = A_{\theta(t)}x(t)\mathrm{d}t + \begin{bmatrix} x(t)'G_{1,\theta(t)}x(t) \\ \vdots \\ x(t)'G_{n,\theta(t)}x(t) \end{bmatrix} \mathrm{d}t + H_{\theta(t)}\mathrm{d}w(t), \quad \forall t \geq 0,\ x(0) = x_0 \in \mathbb{R}^n, \quad (1)$$

where $x(t)$ denotes an n-dimensional system state, $w(t)$ denotes a standard r-dimensional Brownian motion, and $\{\theta(t)\}$ represents an irreducible continuous-time Markov process having $\mathscr{S} = \{1, \ldots, N\}$ as state space. As usual, $x(t)$, $w(t)$, and $\theta(t)$ are mutually independent random variables at $t \geq 0$. The value of each tuple of matrices $(A_i, H_i, G_{1,i}, \ldots, G_{n,i})$, $i = 1, \ldots, N$, is given.

The main contribution of this paper is to present conditions to assure that the quadratic Markov jump system in (1) is second moment stable, as follows.

Definition 1.1. *([1, Defn. 11.3.1, p. 188]). We say the quadratic Markov jump system in* (1) *is second moment stable if there exists some constant $c = c(x_0)$ such that*

$$\mathrm{E}[\|x(t)\|^2] \leq c, \quad \forall t \geq 0.$$

Now, consider the elements of the n-dimensional vector $x(t)$ written explicitly in the form $x(t) \equiv [x_{[1]}(t), \ldots, x_{[n]}(t)]'$.

Assumption 1.1. *The elements $x_{[\ell]}(t)$, $\ell = 1, \ldots, n$, are uniformly bounded from below almost surely. As a result, there exist values $\mu_1, \ldots, \mu_n$ such that*

$$\mu_\ell \leq \liminf_{t\to\infty} x_{[\ell]}(t), \quad \ell = 1, \ldots, n, \quad (2)$$

almost surely.

The condition in Assumption 1.1 is fundamental in our approach. Assumption 1.1 states a lower bound for $x_{[\ell]}(t)$, but an upper bound on $x_{[\ell]}(t)$ may not exist, that is, $x_{[\ell]}(t)$ could diverge to infinity as t goes to infinity. In order to prevent such divergent behaviour in (1), we present conditions to guarantee the second moment stability, as in Definition 1.1.

The assumption that $x_{[\ell]}(t)$ has a lower bound is mild, since there are many applications for which the system states are bounded from below. For instance, in DC motors, both the angular velocity and the electrical current are bounded from below [19, 20].

This paper has two contributions. First, the paper shows conditions to assure the second moment stability of the quadratic system in (1). Second, the paper shows a practical application to an electrical circuit based on resistor (R), inductor (L), and capacitor (C).

RLC circuits have the electrical current and the voltage as elements of the system-state—the lower-bounds required by Assumption 1.1 arise from circuits' assemblage, as illustrated in Section 4. Indeed, we used our theoretical result to design a stabilizing Markov jump controller for an RLC circuit in practice. Experiments were carried out, and the corresponding experimental data support our findings.

The paper is organized as follows. Section 2 quotes the notation, definitions, and Section 3 presents the main stability result for the stochastic system (1). Section 4 illustrates our findings through a real-time application for an RLC circuit. Finally, Section 5 presents some concluding remarks.

2. Notation and definitions

Let us denote the n-dimensional Euclidean space by $\mathbb{R}^n$ and the corresponding Euclidean norm by $\|\cdot\|$. The symbol $\mathrm{tr}\{\cdot\}$ denotes the trace operator. The identity matrix on $\mathbb{R}^{n\times n}$ is represented by I_n. The symbol $\mathbb{1}_{\mathcal{C}}$ represents the Dirac measure of $\mathcal{C}$, i.e., $\mathbb{1}_{\mathcal{C}}$ equals 1 when the condition $\mathcal{C}$ is true and 0 otherwise. Given two matrices $U \in \mathbb{R}^{n\times n}$ and $V \in \mathbb{R}^{m\times m}$, $\mathrm{diag}(V, U)$ represents a square diagonal matrix made up by V and U as entries in its diagonal form. For simplicity, we use the notation $\mathrm{diag}(V_i)_{\{i=1,\ldots,N\}}$ to represent $\mathrm{diag}(V_1, \ldots, V_N)$.

Let $\otimes$ be the Kronecker product in such a way that $U \otimes V \in \mathbb{R}^{nm\times nm}$ is the corresponding Kronecker matrix [4]. The Kronecker sum is defined as $U \oplus V = U \otimes I_m + I_n \otimes V$. Let $\mathrm{Re}(z)$ denote the real part of the complex number z. Given any matrix $U \in \mathbb{R}^{n\times n}$, $\sigma(U)$ represents the spectrum of U; and the largest real part of the eigenvalues of U is referred to as

$$\mathrm{Re}(\lambda_U) := \max\{\mathrm{Re}(\lambda) : \lambda \in \sigma(U)\}.$$

When U stands for a set of N matrices, i.e. $U = (U_1, \ldots, U_N)$, we apply the definition

$$\mathrm{Re}(\lambda_U) = \max\left\{\mathrm{Re}(\lambda_{U_i}), i = 1, \ldots, N\right\}.$$

3. Main result

The main result of this paper is presented in the sequence.

Let $\Pi = [\pi_{ij}], i, j = 1, \ldots, N$ be the transition rate matrix associated with the Markov process $\{\theta(t)\}$. Accordingly, consider $p_i(t) := P(\theta(t) = i)$, $i = 1, \ldots, N$, $\forall t \geq 0$. Consider the second moment matrix

$$X_i(t) = \mathrm{E}[x(t)x(t)'\mathbb{1}_{\theta(t)=i}], \quad i = 1, \ldots, N, \quad \forall t \geq 0. \tag{3}$$

Consider also the symmetric positive semidefinite matrix $V(t) \in \mathbb{R}^{n\times n}$, solution of the matrix differential equation

$$\dot{V}_i(t) = V_i(t)\left(A_i + \sum_{\ell=1}^{n} \mu_\ell G_{\ell,i}\right)' + \left(A_i + \sum_{\ell=1}^{n} \mu_\ell G_{\ell,i}\right) V_i(t) + \sum_{j=1}^{N} \pi_{ji} V_j(t) + H_i H_i' p_i(t), \quad i = 1, \ldots, N, \quad \forall t \geq t_0, \tag{4}$$

with an initial condition $V_i(t_0) \in \mathbb{R}^{n\times n}$, for each $i = 1, \ldots, N$.

Now, we are able to present the main result of this paper.

Theorem 3.1. *Assume that the matrices $G_{1,i}, \ldots, G_{n,i}$, $i = 1, \ldots, N$, are negative semi-definite. Then there exists some $t_0 \geq 0$ such that*

$$\operatorname{tr}\{X_i(t)\} \leq \operatorname{tr}\{V_i(t)\}, \quad i = 1, \ldots, N, \quad \forall t \geq t_0, \tag{5}$$

where $V(t)$ satisfies (4) with $V(t_0) = X(t_0)$.

The proof of Theorem 3.1 is available in Appendix.

Remark 3.1. *Theorem 3.1 assures that $X(t)$ is bounded from above by $V(t)$, for all $t \geq t_0$. Due to $\mathrm{E}[\|x(t)\|^2] = \operatorname{tr}\{\mathrm{E}[x(t)x(t)']\} = \sum_{i=1}^{N} \operatorname{tr}\{X_i(t)\}$, we can conclude that the Markov jump quadratic system in (1) is second moment stable provided that $V(t)$ is uniformly bounded. This conclusion represents the main theoretical novelty of this paper.*

The authors of [11, Thm 5.6], [7, Thm. 3.25, p. 52] have introduced a condition that we recall here to check whether $V(t)$ is uniformly bounded. To present such a condition, we define the matrix

$$\mathcal{A} = \Pi' \otimes I_{n^2} + \operatorname{diag}\left(\left(A_i + \sum_{\ell=1}^{n} \mu_\ell G_{\ell,i}\right) \oplus \left(A_i + \sum_{\ell=1}^{n} \mu_\ell G_{\ell,i}\right)\right)_{\{i=1,\ldots,N\}}. \tag{6}$$

Proposition 3.1. *([11, Thm 5.6], [7, Thm. 3.25, p. 52]). If $\operatorname{Re}(\lambda_{\mathcal{A}}) < 0$, then the limit $\lim_{t\to\infty} V(t)$ in (4) does exist and does not depend on the initial condition $V(t_0) \in \mathbb{R}^{n\times n}$.*

The existence of $\lim_{t\to\infty} V(t)$ assures that $V(t)$ is uniformly bounded. This conclusion, together with Theorem 3.1, Remark 3.1, and Proposition 3.1, allows us to present the next result.

Corollary 3.1. *Let the matrices $G_{1,i}, \ldots, G_{n,i}$, $i = 1, \ldots, N$, be negative semi-definite. If $\operatorname{Re}(\lambda_{\mathcal{A}}) < 0$, then the quadratic Markov jump system in (1) is second moment stable.*

Remark 3.2. *The novelty of Corollary 3.1 is that it reveals a easy-to-check condition to verify the second moment stability of the quadratic system in (1), i.e., $\operatorname{Re}(\lambda_{\mathcal{A}}) < 0$, a condition borrowed from [11, Thm 5.6], [7, Thm. 3.25, p. 52]. Thus, Corollary 3.1 expands the use of the matrix (6) for Markov jump systems with quadratic terms.*

Remark 3.3. *Corollary 3.1 has practical implications to design a real-time controller subject to Markov jumps in an RLC circuit, where the corresponding experimental data confirm the usefulness of Corollary 3.1, as detailed in Section 4.*

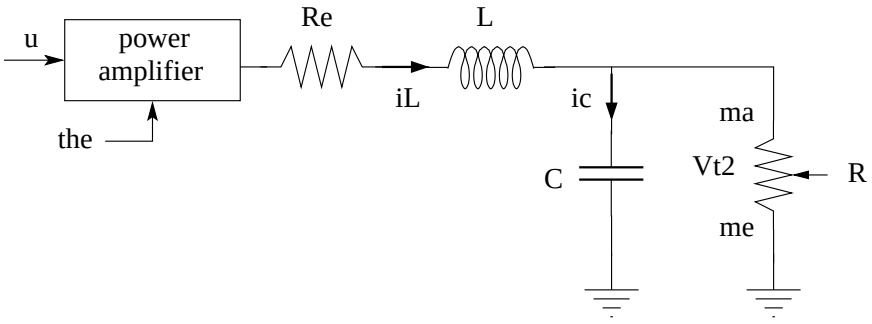

Figure 1: Open-loop diagram of the RLC circuit. The Markov chain generates jumps for both the power amplifier and the resistive load $R_{\theta(t)}$.

4. RLC circuit with Markov-driven load

Circuits based on resistor (R), inductor (L), and capacitor (C) are widely used in electrical equipments, such as antennas [2, 12], power converters [10, 13], filters [8], and oscilators [15]. In many of these applications based on RLC circuits, the load changes as the time evolves.

When electronic elements are connected or disconnected from the load terminals, the nominal value of the load changes accordingly. As such, time-varying loads induce time-varying voltages in the load terminals; but voltage fluctuations in terminals may represent risks of damage for the underlying devices. It is then necessary to keep the voltage supplied to the load at a fixed, regulated level.

The main contribution of this section is that of applying Corollary 3.1 to design a real-time controller for the RLC circuit. The aim of the controller is to regulate the voltage supplied to the load—the load value jumps according to a Markov chain. Actually, the proposed controller depends on quadratic terms. The benefits of such controller become clear through real-time experiments, as detailed next.

4.1. Modelling the RLC circuit with Markov jumps in the load

The RLC circuit studied in this section is detailed in Fig. 1. As can be seen, the RLC circuit has a power amplifier that converts the input signal $u(t)$ into the voltage-current required to supply the circuit. The output voltage, $v_o(t)$, is applied in the load $R_{\theta(t)}$; and the load $R_{\theta(t)}$ changes its value according to a Markov chain. In fact, three distinct resistive loads were used in the experiments, and the jumps among them were implemented through relays that were programmed to follow a three-state Markov chain.

To model the RLC circuit shown in Fig. 1, we consider a second-order system with two state variables (cf., [30]): (i) the current $i_L(t)$ flowing through the inductor; and (ii) the voltage $v_o(t)$ available in the terminals of the capacitor. It allows us to represent the RLC circuit through the next Markov jump system:

$$\mathrm{d}\begin{bmatrix} v_o(t) \\ i_L(t) \end{bmatrix} = \begin{bmatrix} -a_{11}^{(i)} & a_{12} \\ -a_{21} & -a_{22}^{(i)} \end{bmatrix} \begin{bmatrix} v_o(t) \\ i_L(t) \end{bmatrix} \mathrm{d}t + \begin{bmatrix} 0 \\ b^{(i)} \end{bmatrix} u(t)\mathrm{d}t + \begin{bmatrix} 0 \\ h \end{bmatrix} \mathrm{d}w(t), \tag{7}$$

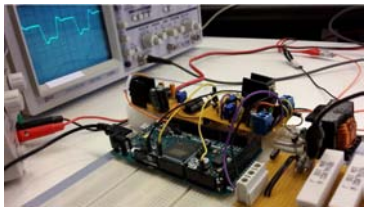

Figure 2: Laboratory testbed used to the experiments involving the RLC circuit.

with $\theta(t) = i \in \{1, 2, 3\}$, for each $t \geq 0$, where $a_{11}^{(i)}, a_{22}^{(i)}, b^{(i)}$, $i = 1, 2, 3$, and a_{12}, a_{21}, h are positive numbers. These numbers were identified by the next procedure.

4.2. Experiments for the identification of the RLC circuit

A laboratory testbed was assembled to carry out the experiments involving the RLC circuit, see Fig. 4.1. The laboratory was equipped with oscilloscopes, microcontrollers, and power sources. A digital oscilloscope (Picoscope Model 2205) was used to measure data from the input-output of the RLC circuit. In its input, the power amplifier received analog signals from an Arduino Due. The Arduino Due was able to generate signals in $u(t)$ from 0V to 2.7V, and it worked with sampling time of 90 microseconds approximately.

In the experiments, the resistor $R_{\theta(t)}$ in the load assumed the value of $30\,\Omega$ when $\theta(t) = 1$, $10\,\Omega$ when $\theta(t) = 2$, and $20\,\Omega$ when $\theta(t) = 3$. Relays were used to implement the jumps among these resistances.

The power amplifier was assembled with an adjustable regulator, code LM338. A phenomenon observed in the laboratory is that the internal resistance of the power amplifier had changed its value slightly when the load changed. This phenomenon suggests that the resistance of the power amplifier was also driven by the Markov jumps; this motivated us to account the influence of such jumps in the element $b^{(i)}$ of the model (7).

In order to identify the parameters of (7), we calculated the mean square error between the model in (7) and the corresponding experimental data (see Fig. 2). Square waves with distinct amplitudes were applied in the input $u(t)$ of the RLC circuit in practice, and the corresponding output data were compared with the values of $v_o(t)$ and $i_L(t)$ taken by simulating (7); this comparison allowed us to find the parameters of (7) that minimized that mean square error—these parameters are shown in Table 1.

4.3. Markov jump control with quadratic terms

Usually, RLC circuits must have a fixed voltage on the load under all operating conditions, voltage condition referred to as *setpoint*. When a Markov jump occurs in the load, the nominal value of the load changes, but changing the load creates a gap between the desired setpoint and the voltage available in the load terminals—this voltage gap is called *offset*.

Voltage offsets are undesired because they can lead not only to unnecessary loss of energy, but also to damage of the underlying equipments. For instance, in transient times, the equipment can suffer voltage spikes, exceeding safety limits. For this reason,

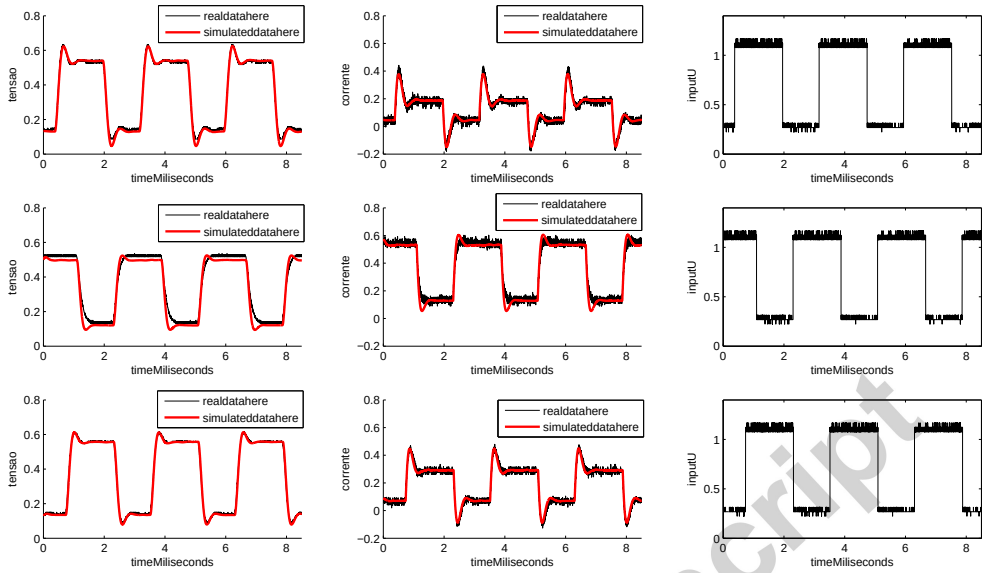

Figure 2: Data from the RLC circuit for a square wave input. Rows from up to down: $\theta(t) \equiv 1$, $\theta(t) \equiv 2$, and $\theta(t) \equiv 3$, respectively. The simulated curves were generated by using the values of Table 1.

it is reasonable to design controllers able to remove that voltage offsets, mainly for RLC circuits with jumping loads. Designing such a controller with the help of Corollary 3.1 sets the main contribution of this section.

The sensors used in the laboratory were designed to measure only the square of the output signals. This signifies that the sensors were used to measure $v_o(t)^2$ and $i_C(t)^2$. This feature lead us to construct a control signal $u(t)$ that depends on $v_o(t)^2$ and $i_C(t)^2$ only, as detailed next.

We mention that the load sensor presented a small bias of -50mV in practice, measured in the laboratory. For this reason, we set $\bar{v}_o(t) = v_o(t) + 0.05$ and adjusted the bias accordingly in $v_o(t)^2$.

Since the Proportional-Integrative (PI) control strategy has produced promising results in the control of processes subject to Markovian jumps [20, 17], we decided to adapt the PI control to our setup, as detailed in the scheme of Fig. 3. Note from Fig. 3 that the

Table 1: Parameters of the quadratic Markov jump system representing an RLC circuit.

Parameters	$i = 1$	$i = 2$	$i = 3$
$a_{11}^{(i)}$	-3.98	-12.2492	-6.01
$a_{22}^{(i)}$	-7.167	-7.012	-8.3177
$b^{(i)}$	6.3415	8.101	7.4757
$a_{12} = 11.495$	$a_{21} = -10.651$	$h = 1$	

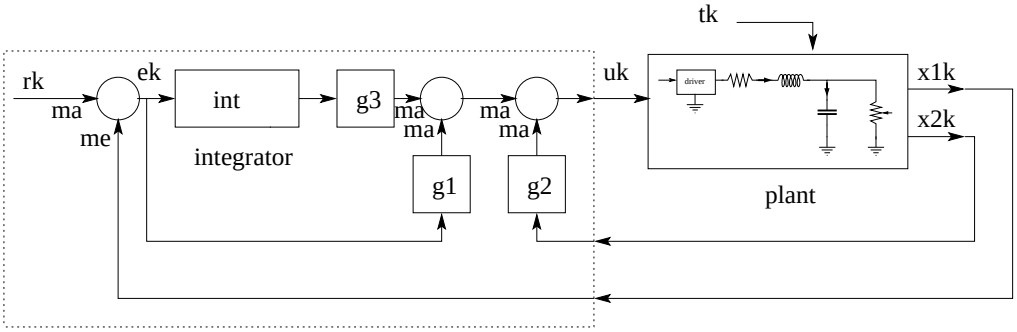

Figure 3: Block representing the 'proportional integrative' (PI) control strategy. The nonlinear feedback accounts both the square of voltage in the load and the square of current in the capacitor.

proposed control action is

$$u(t) = k_1 e(t) + k_2 \int_0^t e(\tau)\mathrm{d}\tau + k_3 i_C(t)^2, \quad e(t) = r(t) - \bar{v}_o(t)^2, \quad \forall t \geq 0, \tag{8}$$

where $r(t)$ stands for a deterministic setpoint signal. With $r(t) \equiv r$, $r > 0$ being a constant to be given latter, the control objective was to assure that the statistical mean values of both $e(t)$ and $i_c(t)$ tend to zero as t tends to infinity.

Due to the Kirchhoff's current law, we can write $i_C(t) = i_L(t) - v_o(t)/R_{\theta(t)}$; hence

$$i_C(t)^2 = \begin{bmatrix} v_o(t) & i_L(t) \end{bmatrix} \begin{bmatrix} \frac{1}{R_{\theta(t)}^2} & \frac{-1}{R_{\theta(t)}} \\ \frac{-1}{R_{\theta(t)}} & 1 \end{bmatrix} \begin{bmatrix} v_o(t) \\ i_L(t) \end{bmatrix}. \tag{9}$$

Now, take the system state as $x(t) \equiv [v_o(t)\ i_L(t)\ q(t)]'$; here $q(t)$ denotes the integral of the error, i.e., $q(t) := \int_0^t e(\tau)\mathrm{d}\tau$, so that $\dot{q}(t) \equiv e(t)$. Combining (7)–(9), we obtain the quadratic Markov jump system (with $\theta(t) = i$):

$$\begin{aligned} \mathrm{d}x(t) = &\begin{bmatrix} -a_{11}^{(i)} & a_{12} & 0 \\ -a_{21} - 0.1 b^{(i)} k_1 & -a_{22}^{(i)} & b^{(i)} k_2 \\ -0.1 & 0 & 0 \end{bmatrix} x(t)\mathrm{d}t + \begin{bmatrix} x(t)' G_{1,i} x(t) \\ x(t)' G_{2,i} x(t) \\ x(t)' G_{3,i} x(t) \end{bmatrix} \mathrm{d}t \\ &+ \begin{bmatrix} 0 \\ b^{(i)} k_1 (r(t) - 0.0025) \\ r(t) - 0.0025 \end{bmatrix} \mathrm{d}t + \begin{bmatrix} 0 \\ h \\ 0 \end{bmatrix} \mathrm{d}w(t), \end{aligned} \tag{10}$$

where

$$G_{1,i} = 0, \quad G_{2,i} = b^{(i)} \begin{bmatrix} k_3/R_i^2 - k_1 & -k_3/R_i & 0 \\ -k_3/R_i & k_3 & 0 \\ 0 & 0 & 0 \end{bmatrix}, \quad G_{3,i} = \mathrm{diag}(-1, 0, 0), \quad i = 1, 2, 3.$$

The controlled RLC circuit with Markov jumps in (10) satisfies the condition stated in Assumption 1.1. Indeed, for the RLC circuit assembled in our laboratory testbed, the output voltage $v_o(t)$ was greater than -1V as well as the current $i_L(t)$ was greater than

-1A for all $t \geq 0$. As a result, in (2), we considered $\mu_1 = -1$ and $\mu_2 = -1$ to cope (2) with (10). To complete the analysis, we have assumed that $\mu_3 = -10$.

The Markov jumps on the load were programmed through relays, which followed the next transition rate matrix:

$$\Pi = \begin{bmatrix} -53.0492 & 42.2072 & 10.8420 \\ 42.2072 & -53.0492 & 10.8420 \\ 54.2098 & 54.2098 & -108.4196 \end{bmatrix}.$$

Corollary 3.1 now plays a key role. In fact, with gains $(k_1, k_2, k_3) = (0.5, 0.05, -0.01)$ arbitrarily chosen, we have that the corresponding matrix $\mathcal{A}$ in (6) yields $\mathrm{Re}(\lambda_{\mathcal{A}}) = -0.0097$. Consequently, Corollary 3.1 assures that the quadratic Markov jump system in (10) is second moment stable.

The remaining part of this section shows data collected from experiments that confirm the second moment stability; this finding corroborates the usefulness of Corollary 3.1 for the RLC circuit.

4.4. Experimental results: controlled RLC circuit with Markov jumps

The controlled RLC circuit with Markov jumps shown in Fig. 3 was assembled in the laboratory testbed with control gains (k_1, k_2, k_3) as mentioned previously.

A small sample of data is shown in Fig. 4. The picture shows the output corresponding to a step from 0V to 0.6V applied at $t = 1.5$ms, or equivalently, the reference was $r(t) = r = 0.36\text{V}^2$ when $t \geq 1.5$ms and zero otherwise. As can be seen in Fig. 4, the controller was able to overcome the perturbations produced by the Markov jumps on the load, driving the load voltage to the setpoint of 0.6V.

To assess the influence of the Markov jumps in the controlled RLC circuit, we analysed the data taken from $12,000$ distinct experiments. Each experiment was carried out for a step from 0V to 0.6V and execution time of 20ms. The experimental data were used to generate the phase portrait depicted in Fig. 5.

Fig. 5 shows data for $12,000$ experiments. Since the jumps in the load produced perturbations for both voltage and current, Fig. 5 represents the statistical dispersion of these perturbations, accounted in the shading of the colors. As can be seen, the statistical dispersion of voltage and current tends to follow an spiral path, in the clockwise direction, and reach an accumulated point in 0.6V and 0A (colored in red in the middle of the picture). This accumulated point represents the statistical mean.

In summary, Fig. 5 suggests that the controlled RLC circuit be second moment stable, an evidence that supports the result of Corollary 3.1—Corollary 3.1 states that the quadratic system in (10) is second moment stable.

Our findings thus reinforce the usefulness of Corollary 3.1 for applications.

5. Concluding remarks

In this paper, we have presented conditions to assure the second moment stability of Markov jump systems with quadratic terms. To prove our main result, we have borrowed from [11, Thm 5.6], [7, Thm. 3.25, p. 52], a condition based on the spectral radius of

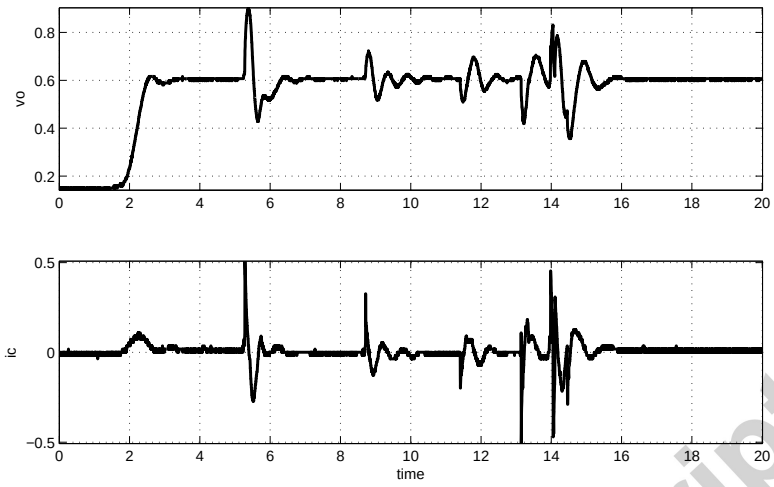

Figure 4: Typical response of the voltage in the load and current in the capacitor from a controlled RLC circuit subject to jumps on the load—the jumps driven by a Markov chain generated the perturbations. Even under perturbations, the proposed controller steered the load voltage to the desired setpoint (i.e., 0.6V).

the matrix in (6); and this condition is reinforced here to assure the stability of quadratic Markov jump systems (see both Assumption 1.1 and Corollary 3.1).

Besides the theoretical contributions, our findings have practical implications. Indeed, we have applied our stability result on the design of a real-time controller for an RLC circuit. The RLC circuit, assembled in a laboratory, supplied a resistive load with values jumping according to a Markov chain. Interestingly, the sensors used in practice to perform the control measured only the square of the corresponding variables (i.e., $v_o(t)^2$ and $i_C(t)^2$ in Fig. 3). This signifies that the control system resulted in a Markov jump system with quadratic terms.

Our main result, Corollary 3.1, was applied on the design of a second moment stabilizing controller for the RLC circuit—the experimental data suggested that the RLC circuit be second moment stable in practice. This evidence matches the theoretical result, a fact that supports the implications of our approach for applications.

Appendix: Proof of Theorem 3.1

In the next result, the notation $o(h)$ denotes an infinitesimal of higher order than h, i.e., $\lim_{h\downarrow 0} o(h)/h$ equals zero.

Proposition 5.1. *([11, Lem. 4.2], [7, Ch. 3]). Assume that $f(t)$ on $\mathbb{R}^{n\times m}$ is $\mathcal{F}_t$-measurable and that $f_i(t) := \mathrm{E}[f(t)\mathbb{1}_{\theta(t)=i}]$ exists. Then $\mathrm{E}[f(t)\mathrm{d}(\mathbb{1}_{\theta(t)=i})] = \sum_{j=1}^{N} \pi_{ji} f_j(t)\mathrm{d}t + o(\mathrm{d}t)$.*

Now, we are able to present the proof of Theorem 3.1.

Proof. (Proof of Theorem 3.1).

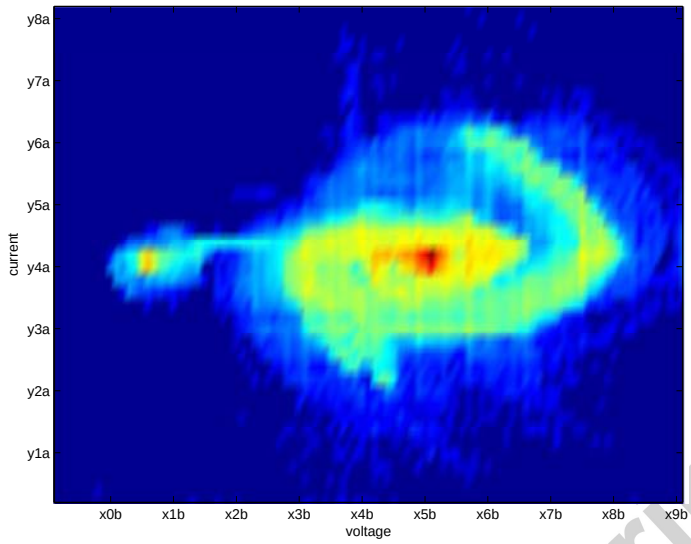

Figure 5: Phase portraits representing the voltage in the load (V) and current in the capacitor (A) measured in practice from a RLC circuit with Markov jumps—the picture condenses data from 12,000 distinct realizations. The picture suggests that the RLC circuit be second moment stable, a fact in accordance with Corollary 3.1.

Before presenting the arguments to prove Theorem 3.1, we need first some definitions. Define the quadratic operator $\mathcal{G}_i : \mathbb{R}^n \mapsto \mathbb{R}^n$, $i = 1, \ldots, N$, as

$$\mathcal{G}_i(x) = \begin{bmatrix} x'G_{1,i}x \\ \vdots \\ x'G_{n,i}x \end{bmatrix}, \quad \forall x \in \mathbb{R}^n. \tag{11}$$

The next argument introduces the matrix differential equation for (3). Indeed, by applying the Itô's rule in (1), we can write $\mathrm{d}X_i(t)$ as (e.g., [7, Prop. 3.28, p. 56])

$$\begin{aligned} \mathrm{d}\,\mathrm{E}[x(t)x(t)'\mathbb{1}_{\theta(t)=i}] &= \mathrm{E}[\mathrm{d}x(t)\,\mathrm{d}x(t)'\mathbb{1}_{\theta(t)=i}] \\ &\quad + \mathrm{E}[\mathrm{d}x(t)\,x(t)'\mathbb{1}_{\theta(t)=i}] + \mathrm{E}[x(t)\,\mathrm{d}x(t)'\mathbb{1}_{\theta(t)=i}] + \mathrm{E}[x(t)x(t)'\,\mathrm{d}(\mathbb{1}_{\theta(t)=i})]. \end{aligned} \tag{12}$$

For the sake of clarity, each term in the right-hand side of (12) is evaluated in separate, as follows. The first term in the right-hand side of (12) reads as

$$\mathrm{E}[\mathrm{d}x(t)\,\mathrm{d}x(t)'\mathbb{1}_{\theta(t)=i}] = \mathrm{E}\left[H_{\theta(t)}\mathrm{d}w(t)\mathrm{d}w(t)'H'_{\theta(t)}\mathbb{1}_{\theta(t)=i}\right] = H_iH'_ip_i(t)\mathrm{d}t. \tag{13}$$

The second term in the right-hand side of (12) is identical to (using notation in (3))

$$\begin{aligned} \mathrm{E}[\mathrm{d}x(t)\,x(t)'\mathbb{1}_{\theta(t)=i}] &= \mathrm{E}\left[\big(A_{\theta(t)}x(t) + \mathcal{G}_{\theta(t)}(x(t))\big)x(t)'\mathbb{1}_{\theta(t)=i}\right]\mathrm{d}t + \mathrm{E}[H_{\theta(t)}\mathrm{d}w(t)x(t)'\mathbb{1}_{\theta(t)=i}] \\ &= A_iX_i(t)\mathrm{d}t + \mathrm{E}[\mathcal{G}_{\theta(t)}(x(t))x(t)'\mathbb{1}_{\theta(t)=i}]\mathrm{d}t. \end{aligned} \tag{14}$$

The last term in the right-hand side of (12) follows from Proposition 5.1, which assures that

$$\mathrm{E}[x(t)x(t)'\,\mathrm{d}(\mathbb{1}_{\theta(t)=i})] = \sum_{j=1}^{N}\pi_{ji}X_j(t)\mathrm{d}t + o(\mathrm{d}t). \tag{15}$$

Combining (12)–(15) yields

$$\dot{X}_i(t) = X_i(t)A_i' + A_iX_i(t) + \sum_{j=1}^{N}\pi_{ji}X_j(t) + H_iH_i'p_i(t) + \mathrm{E}\left[x(t)\mathcal{G}_{\theta(t)}(x(t))'\mathbb{1}_{\theta(t)=i}\right] + \mathrm{E}\left[\mathcal{G}_{\theta(t)}(x(t))x(t)'\mathbb{1}_{\theta(t)=i}\right]. \quad (16)$$

Note that the trace of the rightmost element of (16) equals

$$\mathrm{tr}\left\{\mathrm{E}\left[\begin{bmatrix} x(t)'G_{1,i}x(t) \\ \vdots \\ x(t)'G_{n,i}x(t)\end{bmatrix}\left[x_{[1]}(t),\ldots,x_{[n]}(t)\right]\mathbb{1}_{\theta(t)=i}\right]\right\}. \quad (17)$$

On the other hand, we have from (2) that given $\varepsilon > 0$, there exists some $t_0 \geq 0$ such that

$$\mu_\ell - \varepsilon < x_{[\ell]}(t), \quad \forall t \geq t_0,\ \ell = 1,\ldots,n.$$

Since the matrix $G_{\ell,i}$ is negative semi-definite by assumption, the value of $x_{[\ell]}(t)x(t)'G_{\ell,i}x(t)$ is bounded from above by $(\mu_\ell - \varepsilon)x(t)'G_{\ell,i}x(t)$ when $t \geq t_0$. Thus, we have from (17) that

$$\mathrm{tr}\left\{\mathrm{E}\left[\mathcal{G}_{\theta(t)}(x(t))x(t)'\mathbb{1}_{\theta(t)=i}\right]\right\} \leq \sum_{\ell=1}^{n}\mathrm{tr}\{\mathrm{E}[(\mu_\ell-\varepsilon)x(t)'G_{\ell,i}x(t)\mathbb{1}_{\theta(t)=i}]\} = \sum_{\ell=1}^{n}\mathrm{tr}\{(\mu_\ell-\varepsilon)G_{\ell,i}X_i(t)\}. \quad (18)$$

Passing the trace operator on both sides of (16), and using (18), we obtain

$$\mathrm{tr}\left\{\dot{X}_i(t)\right\} \leq \mathrm{tr}\left\{X_i(t)\left(A_i + \sum_{\ell=1}^{n}(\mu_\ell-\varepsilon)G_{\ell,i}\right)' + \left(A_i + \sum_{\ell=1}^{n}(\mu_\ell-\varepsilon)G_{\ell,i}\right)X_i(t) + \sum_{j=1}^{N}\pi_{ji}X_j(t) + H_iH_i'p_i(t)\right\}. \quad (19)$$

With $V(t)$ as in (4), $V(t_0) = X(t_0)$, we obtain $\mathrm{tr}\{X_i(t)\} \leq \mathrm{tr}\{V_i(t)\}$, for $i = 1,\ldots,N$, since $\varepsilon > 0$ was taken arbitrarily. The result then follows from (4) and (19). □

[1] Arnold, L., 1974. Stochastic differential equations: Theory and applications. Wiley-Interscience, Hoboken, NJ, USA.

[2] Best, S. R., Kaanta, B. C., 2009. A tutorial on the receiving and scattering properties of antennas. IEEE Antennas and Propagation Magazine 51 (5), 26–37.

[3] Boukas, E. K., 2006. Stochastic Switching Systems: Analysis and Design. Birkhäuser, Boston, USA.

[4] Brewer, J. W., 1978. Kronecker products and matrix calculus in system theory. IEEE Transactions on Circuits and Systems 25 (9), 772–781.

[5] Costa, E. F., Vargas, A. N., do Val, J. B. R., 2011. Quadratic costs and second moments of jump linear systems with general Markov chain. Math. Control Signals Systems 23 (1), 141–157.

[6] Costa, O. L. V., de Oliveira, A., 2012. Optimal mean-variance control for discrete-time linear systems with Markovian jumps and multiplicative noises. Automatica 48 (2), 304–315.

[7] Costa, O. L. V., Fragoso, M. D., Todorov, M. G., 2013. Continuous-Time Markov Jump Linear Systems. Series: Probability and Its Applications. Springer-Verlag, New York.

[8] Deliyannis, T., Sun, Y., Fidler, J. K., 1998. Continuous-Time Active Filter Design (Electronic Engineering Systems). CRC Press, Boca Raton, FL, USA.

[9] Dragan, V., Morozan, T., Stoica, A., 2004. H2 optimal control for linear stochastic systems. Automatica 40 (7), 31103–1113.

[10] Erickson, R. W., Maksimovic, D., 2001. Fundamentals of Power Electronics. Springer, New York, USA.

[11] Fragoso, M., Costa, O., 2005. A unified approach for stochastic and mean square stability of continuous-time linear systems with Markovian jumping parameters and additive disturbances. SIAM J. Control Optim. 44 (4), 1165–1191.

[12] Galehdar, A., Thiel, D. V., O'Keefe, S. G., 2007. Antenna efficiency calculations for electrically small, RFID antennas. IEEE Antennas and Wireless Propagation Letters 6, 156–159.

[13] Inam, W., Afridi, K. K., Perreault, D. J., 2014. High efficiency resonant DC/DC converter utilizing a resistance compression network. IEEE Trans. Power Electronics 29 (8), 4126–4135.

[14] Khasminskii, R. Z., Zhu, C., Yin, G., 2007. Stability of regime-switching diffusions. Stochastic Processes and their Applications 117 (8), 1037–1051.

[15] Lee, T. H., Hajimiri, A., 2000. Oscillator phase noise: a tutorial. IEEE Journal of Solid-State Circuits.

[16] Oliveira, R. C. L. F., Vargas, A. N., do Val, J. B. R., Peres, P. L. D., 2009. Robust stability, H2 analysis and stabilisation of discrete-time Markov jump linear systems with uncertain probability matrix. Internat. J. Control 82 (3), 470 – 481.

[17] Oliveira, R. C. L. F., Vargas, A. N., do Val, J. B. R., Peres, P. L. D., 2014. Mode-independent H2-control of a DC motor modeled as a Markov jump linear system. IEEE Trans. Control Systems Tech. 22 (5), 1915–1919.

[18] Shen, M., Yang, G.-H., 2012. H2 state feedback controller design for continuous Markov jump linear systems with partly known information. Int. J. Systems Science 43 (4), 786–796.

[19] Vargas, A. N., Bortolin, D. C., Costa, E. F., do Val, J. B. R., 2015. Gradient-based optimization techniques for the design of static controllers for Markov jump linear systems with unobservable modes. Int. J. Numer. Model. 28 (3), 239–253.

[20] Vargas, A. N., Costa, E. F., do Val, J. B. R., 2013. On the control of Markov jump linear systems with no mode observation: application to a DC motor device. Int. J. Robust Nonlinear Control 23 (10), 1136–115.

[21] Vargas, A. N., Furloni, W., do Val, J. B. R., 2013. Second moment constraints and the control problem of Markov jump linear systems. Numer. Linear Algebra Appl. 20 (2), 357–368.

[22] Xiong, J., Lam, J., Gao, H., Ho, D. W. C., 2005. On robust stabilization of Markovian jump systems with uncertain switching probabilities. Automatica 41 (5), 897 – 903.

[23] Yin, G., Xi, F., 2010. Stability of regime-switching jump diffusions. SIAM Journal on Control and Optimization 48 (7), 4525–4549.

[24] Yin, G. G., Zhu, C., 2010. Hybrid Switching Diffusions: Properties and Applications. Series: Stochastic Modelling and Applied Probability. Springer, New York, USA.

[25] Yin, Y., Shi, P., Liu, F., Lim, C. C., 2014. Robust control for nonhomogeneous markov jump processes: An application to {DC} motor device. Journal of the Franklin Institute 351 (6), 3322 – 3338.
URL http://www.sciencedirect.com/science/article/pii/S0016003214000866

[26] Zhang, L., 2009. H_∞ estimation for discrete-time piecewise homogeneous Markov jump linear systems. Automatica 45 (11), 2570–2576.

[27] Zhang, L., Gao, H., Kaynak, O., 2013. Network-induced constraints in networked control systems – a survey. IEEE Trans. Industrial Informatics 9 (1), 403–416.

[28] Zhang, L., Lam, J., 2010. Necessary and sufficient conditions for analysis and synthesis of Markov jump linear systems with incomplete transition descriptions. IEEE Trans. Automatic Control 55 (7), 1695–1701.

[29] Zhang, L., Wang, C., Chen, L., 2009. Stability and stabilization of a class of multimode linear discrete-time systems with polytopic uncertainties. IEEE Transactions on Industrial Electronics 56 (9), 3684–3692.

[30] Zhao, X., Zhang, L., Shi, P., Karimi, H. R., 2014. Robust control of continuous-time systems with state-dependent uncertainties and its application to electronic circuits. IEEE Trans. Industrial Electronics 61 (8), 4161–4170.

[31] Zhao, Y., Gupta, V., 2015. Feedback stabilization of Bernoulli jump nonlinear systems: A passivity-based approach. IEEE Transactions on Automatic Control 60 (8), 2254–2259.

[32] Zhu, C., Yin, G., 2007. Asymptotic properties of hybrid diffusion systems. SIAM Journal on Control and Optimization 46 (4), 1155–1179.